Review Article

Journal of Molecular Microbiology and Biotechnology

J Mol Microbiol Biotechnol 2016;26:29–44
DOI: 10.1159/000441656

Published online: March 10, 2016

Structure and Function of Benzylsuccinate Synthase and Related Fumarate-Adding Glycyl Radical Enzymes

Johann Heider[a] Maciej Szaleniec[d] Berta M. Martins[c] Deniz Seyhan[a]
Wolfgang Buckel[a, b] Bernard T. Golding[e]

[a]Laboratory of Microbial Biochemistry, LOEWE Center for Synthetic Microbiology, Philipps University Marburg, and [b]Max-Planck-Institut für terrestrische Mikrobiologie, Marburg, and [c]Institut für Biologie, Strukturbiologie/Biochemie, Humboldt-Universität zu Berlin, Berlin, Germany; [d]Jerzy Haber Institute of Catalysis and Surface Chemistry, Polish Academy of Sciences, Kraków, Poland; [e]School of Chemistry, Newcastle University, Newcastle upon Tyne, UK

Key Words
Benzylsuccinate synthase · Fumarate-adding enzyme · Glycyl radical · Toluene · Alkane · Anaerobic toluene degradation

Abstract
The pathway of anaerobic toluene degradation is initiated by a remarkable radical-type enantiospecific addition of the chemically inert methyl group to the double bond of a fumarate cosubstrate to yield *(R)*-benzylsuccinate as the first intermediate, as catalyzed by the glycyl radical enzyme benzylsuccinate synthase. In recent years, it has become clear that benzylsuccinate synthase is the prototype enzyme of a much larger family of fumarate-adding enzymes, which play important roles in the anaerobic metabolism of further aromatic and even aliphatic hydrocarbons. We present an overview on the biochemical properties of benzylsuccinate synthase, as well as its recently solved structure, and present the results of an initial structure-based modeling study on the reaction mechanism. Moreover, we compare the structure of benzylsuccinate synthase with those predicted for different clades of fumarate-adding enzymes, in particular the paralogous enzymes converting *p*-cresol, 2-methylnaphthalene or *n*-alkanes.

Anaerobic Toluene Degradation

Hydrocarbons were long believed to be resistant to microbial degradation in the absence of oxygen. It was therefore surprising to find that many bacteria degrade these compounds anaerobically [Aeckersberg et al., 1991; Dolfing et al., 1990; Rabus et al., 1993; Vogel and Grbic-Galic, 1986; Zeyer et al., 1986]. After the initial reports dating from 1986, the degradation pathways employed by these bacteria remained enigmatic for a decade. However, over the last 20 years, various oxygen-independent reactions have been characterized for the activation of diverse hydrocarbon substrates, depending on the organism and the respective hydrocarbon [Booker, 2009; Foght, 2008; Fuchs et al., 2011; Heider, 2007; Heider and Schühle, 2013; Rabus et al., 2014]. In the case of anaerobic toluene degradation, a number of competing hypothetical mechanisms have been proposed as potential initiating reactions [Altenschmidt and Fuchs, 1991; Evans et al., 1992; Frazer et al., 1995; Rabus and Widdel, 1995; Seyfried et al., 1994; Zeyer et al., 1986], culminating in the discovery of a novel biochemical reaction generating benzylsuccinate, a C4 adduct of toluene, by the addition of a fumarate cosubstrate to the methyl group of toluene [Beller and Spormann, 1997a, b; Biegert et al., 1996]

KARGER

E-Mail karger@karger.com
www.karger.com/mmb

1464–1801/16/0263–0029$39.50/0

Johann Heider
Laboratory of Microbial Biochemistry, Philipps University of Marburg
Karl-von-Frisch-Strasse 8
DE–35043 Marburg (Germany)
E-Mail heider@biologie.uni-marburg.de

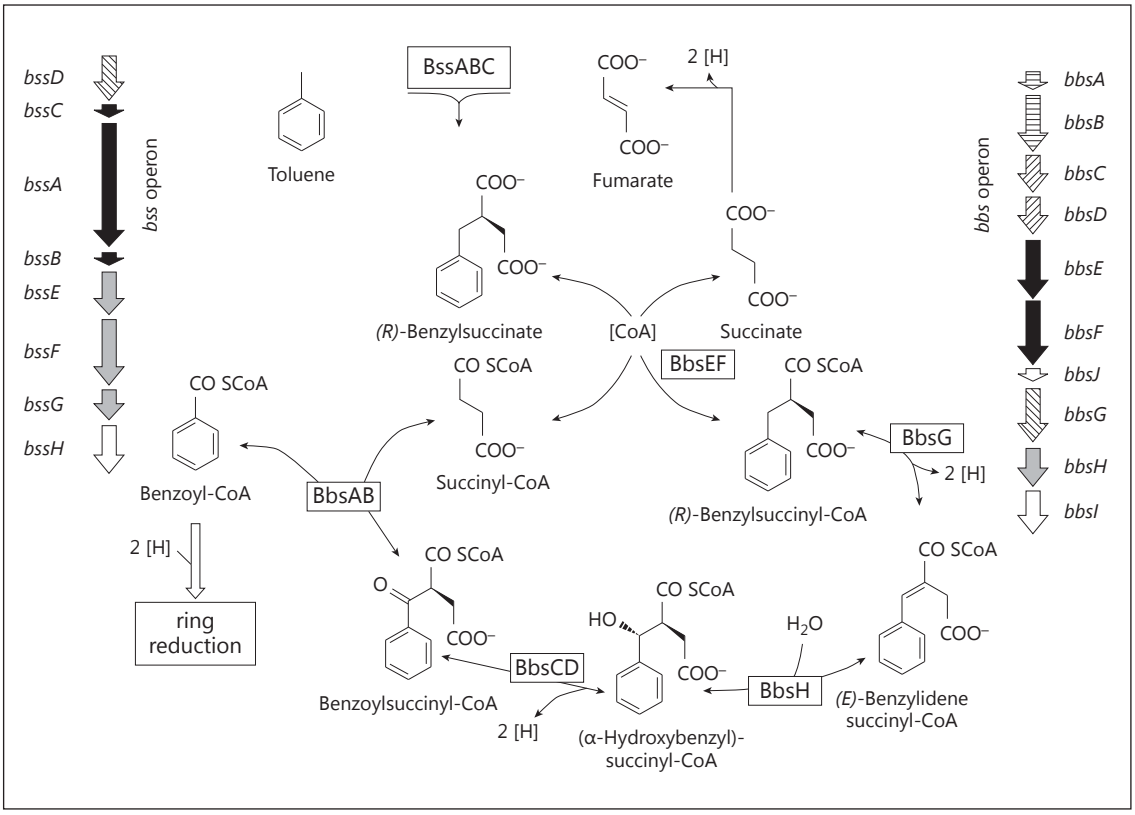

Fig. 1. Anaerobic toluene metabolic pathway and gene organization. The reactions of benzylsuccinate synthase (BssABC) and the enzymes of the further β-oxidation pathway are indicated by the respective gene products. Arrows indicate the reversibility or irreversibility of the respective steps. The operon organization of the *bss* and *bbs* operons are indicated in the left and right margins, respectively. Functions of the gene products are indicated by different hatching patterns. The indicated 2-*(S)*, 3-*(R)*-enantiomeric structure of the 3-hydroxyacyl-CoA intermediate has been implicated by recent structural studies on BbsH and BbsCD [Essen and Heider, unpubl. data]. Gray: universally conserved genes in *bss* operons with unknown function; white: probably nonessential genes of unknown function.

(fig. 1). Benzylsuccinate has previously been observed as excreted metabolite in supernatants of many toluene-degrading anaerobes, but was regarded as dead-end metabolite indicative of other metabolic pathways because it did not support growth of any known anaerobic toluene degrader [Beller et al., 1992; Evans et al., 1992; Frazer et al., 1995; Seyfried et al., 1994]. The role of benzylsuccinate as a true intermediate in anaerobic toluene metabolism and the necessity of a fumarate cosubstrate were first demonstrated by in vitro experiments with extracts of the denitrifying bacterium *Thauera aromatica* [Biegert et al., 1996]. These findings were confirmed with toluene-degrading strains affiliated to the closely related genera *Azoarcus* and *Aromatoleum*, sulfate-reducing strains affiliated to the genus *Desulfobacula* and the anoxygenic phototroph *Blastochloris sulfoviridis* [Beller and Spormann, 1997a, b; Rabus and Heider, 1998; Zengler et al., 1999]. Subsequently, the reaction was shown to be stereospecific as *(R)*-benzylsuccinate was exclusively generated [Beller and Spormann, 1998; Leutwein and Heider, 1999]. The enzyme catalyzing the formation of this compound was identified as a new type of glycyl radical enzyme (GRE), which was called benzylsuccinate synthase (BSS) [Beller and Spormann, 1999; Leuthner et al., 1998]. At the time of its discovery, BSS was only the third type of GRE with a known function, akin to pyruvate formate lyase (Pfl) [Knappe and Sawers, 1990] and anaerobic ribonucleotide reductase [Eklund and Fontecave, 1999; Reichard, 1997]. Today, three more types of GREs with known functions are anaerobic coenzyme B_{12}-independent diol dehydratases [O'Brien et al., 2004; Raynaud et al., 2003], choline trimethylamine ly-

ases [Craciun and Balskus, 2012; Craciun et al., 2014] and 4-hydroxyphenylacetate or indoleacetate decarboxylases [Selmer and Andrei, 2001; Selvaraj et al., this vol., pp. 76–91], as well as a growing subfamily of BSS-like fumarate-adding enzymes (FAEs) involved in the anaerobic degradation of various other chemically inert substrates (see below).

The downstream pathway of anaerobic toluene metabolism was also identified in *T. aromatica* and consists of a modified β-oxidation route (fig. 1), which has been investigated by biochemical and molecular biological methods. All enzymes of this pathway are encoded by the common, toluene-induced *bbs* operon (for β-oxidation of benzylsuccinate) [Leuthner and Heider, 2000], which has been identified in all studied anaerobic toluene degraders (fig. 1). Further degradation of *(R)*-benzylsuccinate starts with its regio- and enantiospecific activation to the CoA thioester 2-*(R)*-benzylsuccinyl-CoA by a specific CoA transferase consisting of two subunits encoded by the *bbsEF* genes [Leuthner and Heider, 2000; Leutwein and Heider, 1999, 2001]. The β-oxidation of benzylsuccinyl-CoA then continues by oxidation to *(E)*-benzylidenesuccinyl-CoA, mediated by benzylsuccinyl-CoA dehydrogenase (BbsG) [Leutwein and Heider, 2002]. This is followed by hydration to the corresponding 3-hydroxyacyl-CoA derivative by the enoyl-CoA hydratase BbsH, oxidation of the alcohol group to the 3-oxoacyl-CoA derivative benzoylsuccinyl-CoA by the alcohol dehydrogenase BbsCD and, finally, a thiolytic cleavage of benzoylsuccinyl-CoA to benzoyl-CoA and succinyl-CoA by the thiolase BbsAB [Leuthner and Heider, 2000] (fig. 1). Benzoyl-CoA is the common intermediate of most anaerobic degradation pathways of aromatic compounds, and the further steps of anaerobic benzoyl-CoA metabolism follow a well-known conserved pathway [Boll et al., this vol., pp. 119–137; Fuchs et al., 2011].

The other known FAE isoenzymes catalyze analogous activation reactions of methyl or methylene groups of recalcitrant substrates and are often associated with enzymes of paralogous β-oxidation pathways, leading to the conversion of alkanes or alkyl-aromatic compounds to acyl-CoA thioesters ready to undergo further reactions. To date, specific FAEs have been described that activate these types of substrates, including *n*-alkanes, cycloalkanes, *p*-cresol, 2-methylnaphthalene, *p*-cymene or ethylbenzene [Callaghan et al., 2006; Kniemeyer et al., 2003, 2007; Musat et al., 2009; Rabus et al., 2001; Selesi et al., 2009; Strijkstra et al., 2014; Wöhlbrand et al., 2013; Jaekel et al., 2015].

Benzylsuccinate Synthase

BSS was first purified and characterized from the Betaproteobacteria *T. aromatica* and *Azoarcus* strain T [Beller and Spormann, 1999; Leuthner et al., 1998]. The enzyme catalyzes the formation of *(R)*-benzylsuccinate, with toluene and fumarate as the only substrates, under strictly anoxic conditions. The enzyme is highly specific for fumarate, which can only be partially replaced by maleate [Beller and Spormann, 1997b; Biegert et al., 1996; Li and Marsh, 2006a, b], but it is still an open question whether maleate actually enters the active site or acts indirectly, for example by inhibiting fumarase in the extracts (or even in the partially purified enzymes), thereby increasing the background fumarate concentration [Biegert et al., 1996]. Conversely, all analyzed enzymes accepted a number of substituted toluene derivatives, such as fluorotoluenes [Biegert et al., 1996], *o*-xylene [Beller and Spormann, 1997b], all three cresol isomers [Verfürth et al., 2004] and *o*-toluidine [Lippert and Heider, unpubl. data]. Interestingly, however, BSS orthologs from different strains vary in their activities for the xylene isomers: BSS of *T. aromatica* strain K172, which degrades toluene but not xylenes, does not convert any xylene isomer to the corresponding succinate adduct, whereas BSS of *Azoarcus* strain T, a known degrader of toluene or *m*-xylene, accepts all xylene isomers as substrates [Krieger et al., 1999; Verfürth et al., 2004]. The same isoenzymes of BSS appear to be often involved in the degradation of toluene and a second substrate (e.g. *m*-xylene for the *Azoarcus* strains or *m*-cresol for *Desulfobacterium cetonicum* or *T. aromatica* strain S100 [Mechichi et al., 2002; Müller et al., 1999]). The ability to grow on these substrates seems to depend mostly on the ability to metabolize the respective succinate adducts [Bozinovski et al., 2014; Juárez et al., 2013].

BSS consists of three subunits of 98, 8.5 and 6.5 kDa, which form an $(\alpha\beta\gamma)_2$ heterohexamer of 220 kDa, as recently verified by the X-ray structure [Funk et al., 2014]. The sequence of the large subunit is similar to that of the catalytic subunits of other GREs, including a conserved Gly residue close to the C-terminus involved in generating and carrying the glycyl radical and a structurally adjacent conserved Cys in the middle of the sequence, which is supposed to be involved in the reaction of all GREs in the form of a reactive thiyl radical (Gly829 and Cys493 for BSS from *T. aromatica*, respectively) [Coschigano et al., 1998; Leuthner et al., 1998; Selmer et al., 2005]. However, the two small subunits are unique for BSS, and other FAEs and are not known from any other enzyme, with the ex-

ception of 4-hydroxyphenylacetate decarboxylase, which contains one additional small subunit [Selmer and Andrei, 2001; Selmer et al., 2005]. It has recently been shown that each of the small subunits of BSS contains a very low-potential Fe_4S_4 cluster of as yet unknown function [Funk et al., 2014; Hilberg et al., 2011; Li and Marsh, 2009], which seems to contribute to the oxygen sensitivity of the enzyme even in the nonactivated form. In comparison, the single small subunit of 4-hydroxyphenylacetate decarboxylase carries two Fe_4S_4 clusters [Martins et al., 2011], but the function of these subunits is unclear in either enzyme. Although the specific activity of BSS is quite low and the available enzyme batches have been largely inactivated during purification, this reaction has been clearly identified as the first step of anaerobic toluene metabolism [Beller and Spormann, 1999; Leuthner et al., 1998].

The presence of a glycyl radical in the activated enzyme has been proven by EPR experiments in the cell extracts of toluene-grown cells [Krieger et al., 2001; Verfürth et al., 2004] and verified by a very high-field EPR study as a distinct glycyl radical type compared to those known in Pfl or anaerobic ribonucleotide reductase [Duboc-Toia et al., 2003]. As with other GREs, activated BSS is immediately and irreversibly inactivated by exposure to oxygen, which results in the cleavage of the large subunit at the site of the radical-carrying Gly residue [Leuthner et al., 1998], giving a characteristic double-band appearance of the large subunit after SDS-PAGE [Beller and Spormann, 1999; Leuthner et al., 1998]. This behavior is typical for all known GREs and has been interpreted as evidence for a 'half-of-the-sites' reactivity of the enzyme, which allows only one of the subunits in the dimeric complexes to be activated to the glycyl radical form [Knappe and Sawers, 1990; Leuthner et al., 1998]. Conversion to the active, radical-containing form of BSS requires an additional activating enzyme, BssD, which is encoded in a common operon with the three subunits of BSS (BssCAB) or any other FAE in every known case [Achong et al., 2001; Coschigano et al., 1998; Kube et al., 2004; Leuthner et al., 1998]. BssD shows a strong similarity to the activating enzymes of other GREs and belongs to the family of S-adenosyl-methionine radical enzymes [Sofia et al., 2001]. It differs from the previously known Pfl and anaerobic ribonucleotide reductase-activating enzymes by containing an additional enzyme domain apparently housing two extra ferredoxin-like Fe_4S_4 clusters of unknown function, a property shared with the activating enzymes connected to the 4-hydroxyphenylacetate decarboxylases and most other GREs [Leuthner et al., 1998; Selmer et al., 2005].

Genetic Organization

The genes coding for BSS and its activating enzyme are organized in a common operon, which was assigned as the *bss* operon (fig. 1) [Achong et al., 2001; Aklujkar et al., 2009; Coschigano et al., 1998; Kube et al., 2004; Leuthner et al., 1998]. The gene order of all known *bss* operons is *bssDCAB*, starting with the gene for the activating enzyme and followed by those for the γ-, α- and β-subunits. Moreover, the known *bss* operons continue with at least two or even more conserved genes of unknown function that have been labeled *bssE*, *bssF*, etc. [Hermuth et al., 2002; Kube et al., 2004] and are also present as paralogs in the gene clusters coding for other FAEs (see below). Together with the *bbs* operon coding for the enzymes of further degradation of benzylsuccinate and a putative operon involved in solvent resistance, the *bss* operon was shown to be exclusively expressed under anoxic conditions in the presence of toluene [Achong et al., 2001; Coschigano, 2000; Hermuth et al., 2002; Kube et al., 2004; Kühner et al., 2005]. This regulation is proposed to be conferred by a two-component system called TdiSR (toluene-degradation inducer) whose genes have been identified next to the *bss* operons of all characterized denitrifying bacteria [Achong et al., 2001; Coschigano and Young, 1997; Heider and Rabus, 2008; Kube et al., 2004; Leuthner and Heider, 1998; Rabus et al., 2005], whereas a XylR-like regulation system may be responsible for regulating these genes in strictly anaerobic toluene degraders such as *Geobacter metallireducens* [Aklujkar et al., 2009; Butler et al., 2007]. Different mRNA starting points of the *bss* operon located either in front of the *bssD* gene for the activating enzyme or in front of *bssC*, the first gene of actual BSS, have been identified for the *bss* operons of *T. aromatica* and *Azoarcus* strain T [Achong et al., 2001; Hermuth et al., 2002]. Based on RNA stability assays with *T. aromatica*, this phenomenon was explained by a putative RNase processing event close to the end of the *bssD* gene followed by rapid degradation of the *bssD*-containing mRNA fragment, while the mRNA segment coding for the subunits of BSS is much more stable [Hermuth et al., 2002]. This was interpreted as a potential mechanism to prevent excessive synthesis of the activating enzyme while still retaining its simultaneous induction with BSS. The transcription studies also showed that the mRNA continues beyond the *bssCAB* genes coding for the subunits of BSS and also covers the additional genes of unknown function [Hermuth et al., 2002; Kube et al., 2004].

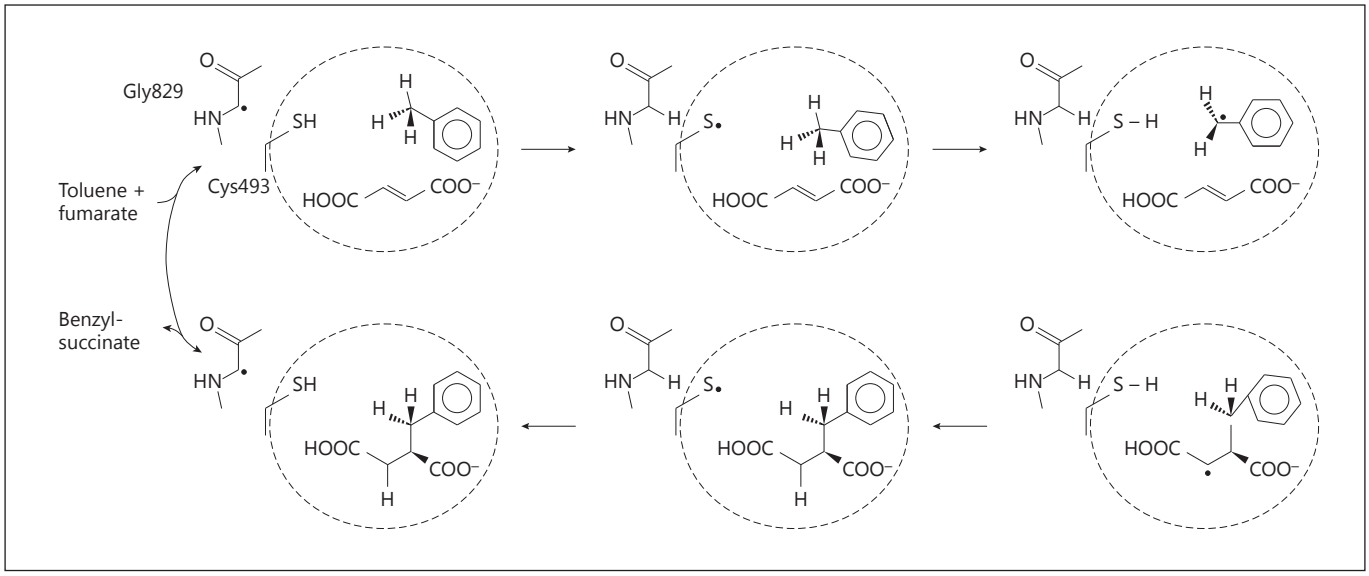

Fig. 2. Proposed reaction mechanism of BSS. The dotted area represents the active site cavity accessible to the substrates.

Mechanism

A schematic catalytic mechanism for generating benzylsuccinate from enzyme-bound toluene and fumarate has been proposed based on the nature of BSS as a GRE [Heider et al., 1998] (fig. 2). Because of the relative stability of glycyl radicals under anaerobic conditions [Buckel and Golding, 2006; Knappe and Sawers, 1990], the activated state of BSS with the radical localized at Gly829 appears to act as a low-reactivity resting state until both substrates are bound in the active site. Because of the high reactivity of the other radical intermediates involved, all following reactions must be expected to occur in a shielded environment of the active site blocked against access of unwanted reactive compounds. The reaction is supposed to be initiated by the glycyl radical-dependent generation of a thiyl radical at the conserved Cys493, which is in close proximity to the active site Gly829, as in all other known GREs [Funk et al., 2014]. The reactive thiyl radical is supposed to abstract a hydrogen atom from the methyl group of toluene, leading to a transient enzyme-bound benzyl radical intermediate. This benzyl radical then attacks the double bond of a fumarate cosubstrate already bound in the active center to form a product-related benzylsuccinyl radical. Finally, the product radical regains the initially abstracted hydrogen from Cys493, restoring it to the thiyl radical state, which can then reestablish the resting glycyl radical state of the enzyme (fig. 2). Only this last step presumably opens the active site for the release of benzylsuccinate and the binding of substrates for the next round of catalysis. The proposed mechanism is supported by studies with isotopically labeled toluene, showing that the initially abstracted hydrogen atom is indeed regained in the product benzylsuccinate [Beller and Spormann, 1999]. Gas-phase density functional theory (DFT) calculations also demonstrated the intrinsic plausibility of the proposed reaction sequence [Himo, 2002, 2005].

A few additional mechanistic details were obtained for the reaction of BSS, starting with the stereospecificity of the reaction, which as mentioned above produces only *(R)*-benzylsuccinate [Beller and Spormann, 1999; Leutwein and Heider, 1999]. Moreover, hydrogen removal from the methyl group seems to be the rate-limiting step, judging by the measured kinetic isotope effects with deuterated toluene, but not fumarate [Li and Marsh, 2006a, b; Seyhan et al., unpubl. data], and the hydrogen abstracted from toluene is donated back to the succinate moiety of benzylsuccinate in a *syn*-addition mechanism (fig. 2) [Qiao and Marsh, 2005]. Finally, recent experiments with toluene containing a chiral methyl group proved that the addition of fumarate to toluene occurs with the inversion of the stereochemistry at the methyl group [Seyhan et al., unpubl. data]. This stereochemical outcome is analogous to the recently identified mode of fumarate addition to a chirally labeled methylene group of *n*-hexane by an FAE involved in anaerobic hexane metabolism [Jarling et al., 2012].

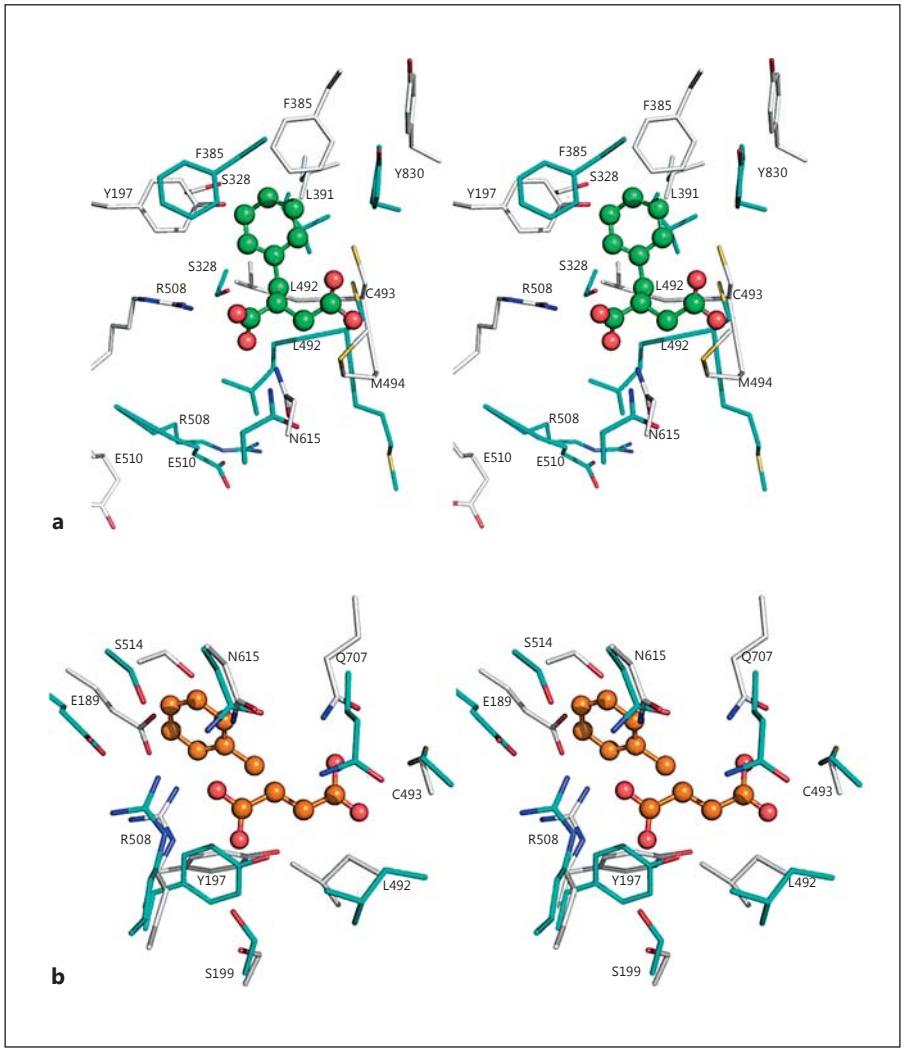

Fig. 3. Stereo-view comparisons of the active site pocket of BSS. Amino acid side chains are shown in stick mode. **a** Comparison of BSS (PDB code 4pkc) with a previously predicted homology protein model [Bharadwaj et al., 2013]. The color code of the reported structure is gray (carbon), red (oxygen), blue (nitrogen) and yellow (sulfur), while the carbon atoms of the homology model are cyan. The modeled reaction product *(R)*-benzylsuccinate from the homology model is shown in green (carbon) and red (oxygen). Except for the amino acids of the Gly829-containing loop (only Tyr830 shown for clarity) and Cys493, all other residues surrounding the active site pocket do not superimpose. The peptide stretch between Leu492-Met494 is shown in ribbon representation to visualize the different conformations adopted by the side chains. **b** Comparison of the active site pockets from the structure of BSS before and after MD/MM (molecular dynamic/molecular mechanical) relaxation to accommodate binding of the substrates [Szaleniec et al., submitted]. The color code for the reported structure is as above, while the carbon atoms of the relaxed protein model are in cyan. Bound fumarate and toluene from the MD/MM calculation are shown in orange (carbon) and red (oxygen). Fumarate is anchored by an extensive network of hydrogen-bonding interactions and a salt bridge with the side chains of Tyr197, Ser199, Arg508, Asn615 and Gln707. The side chains of Glu189, Tyr381 (not shown) and Ser514 are displaced to allow binding of toluene.

Structure of BSS and Structure-Based Mechanistic Models

Structural Features of BSS

The first X-ray structure of a BSS has recently been reported [Funk et al., 2014] and confirmed the predicted composition as a $(\alpha\beta\gamma)_2$ heterohexamer of the three subunits. The structure shows that the small subunits indeed contain Fe_4S_4 clusters ligated by four conserved cysteines which structurally resemble the arrangements found in high-potential iron proteins. However, the small subunits are located on the surface of the enzyme and appear to be far away from the catalytic center, although the β-subunit has been proposed to play a potential role in controlling substrate access [Funk et al., 2014]. The α-subunit showed a typical fold to that found in other GREs, forming a 10-stranded β-barrel enclosing two loops, which contain the catalytic residues Gly829 and Cys493 at their respective tips. Among these functionally important amino acids, only Cys493 has access to an active site cavity proposed to be involved in the binding of the substrates. A chloride ion bound in close proximity to Cys493 was proposed to be a potential analog of one of the carboxyl groups of fumarate, while the second carboxyl group was proposed to interact with the universally conserved Arg508 side chain present in all known FAEs (see below). Moreover, the other side of the apparent active site cavity was reported to be lined by hydrophobic amino acids that may accomplish toluene binding [Funk et al., 2014].

Mechanistic Modeling

In the absence of structural information on BSS, a homology protein model has been constructed for a structure-based analysis of the reaction mechanism [Bharadwaj et al., 2013]. However, the recently published structure of BSS shows many deviations around the active site, as shown by comparing the predicted and the reported crystal structures (fig. 3a), rendering any conclusions drawn from this study as highly doubtful. Therefore, the reaction mechanism of BSS was recently reevaluated using DFT on a cluster model based on the actual structure of the α-subunit from the crystallographic data (Protein Data Bank, PDB code: 4pkf) [Funk et al., 2014]. The model was obtained in a four-step procedure as follows: (1) docking the product *(R)*-benzylsuccinate into the active site cavity, (2) relaxation of the structure of the enzyme-product complex by molecular dynamics, (3) construction and geometry optimization of the enzyme-substrate complex (with both fumarate and toluene bound) based on the optimal geometry of the previously obtained enzyme-product complex (fig. 3b) and (4) selection of residues for the QM (quantum mechanical) cluster model of the active site to be used in DFT modeling [Szaleniec et al., submitted]. The docking studies indicated that fumarate is most effectively bound with a charged COO^- group extending towards the positively charged Arg508 residue. The resulting QM cluster model contained whole or fragmented side chains of nine active site amino acids surrounding the bound substrates (Glu189, Tyr197, Ser199, Ile384, Leu391, Leu492, Cys493, Arg508, and Val709: 147 atoms in total) with added geometry constraints. These constraints were introduced to mimic the structural settings of the rest of the enzyme and to ensure that the selected active-site residues were still held in appropriate positions after cutting their side chains from the protein backbone.

The QM cluster model obtained was used to study different variants of the proposed reaction mechanism [Himo, 2002; Li and Marsh, 2006b] as well as to probe factors imposed by the stereospecificity of the reaction. The DFT study confirmed the viability of the generally accepted reaction hypothesis, that is, an initial attack of the reactive thiyl radical of Cys493 on the methyl group of toluene, followed by the formation of a C-C bond between the generated benzyl radical and fumarate, and finally quenching of the benzylsuccinyl radical intermediate by a back transfer of an H atom from Cys493. The results of this study yielded significant changes in the relative heights of the energetic barriers associated with the elementary steps of the mechanism, which were introduced by the steric constraints imparted by the enzyme active site (fig. 4). Previous calculations on the mechanism were performed by gas-phase studies and proposed that the step of C-C bond formation (TS2) would be rate limiting [Himo, 2002, 2005]. Based on the new modeling study it can be inferred that C-H activation (TS1) controls the reaction rate, and the calculated barriers for TS1 and TS2 differ by 4.8 kcal/mol (fig. 4). The quenching step for the product radical (TS3) seems to control the regioselectivity of the reaction, that is, a preferential attack of the benzyl radical on the distal C3 atom of fumarate (relative to Cys493). While the TS barriers for attacking either atom of the double bond are virtually identical, the barrier for quenching the benzylsuccinate radical by abstracting a hydrogen from Cys493 is very high for the wrong regioisomer (approx. 50 kcal/mol), as it requires breaking the strong salt brigde with Arg508 (<3 Å distance) and additional hydrogen bonds (fig. 3b). If the C-C bond is formed with C3 of fumarate, all reagents remain in place during radical quenching, and substantial repositioning effects are avoided. Therefore, even if the wrong radical intermediate should be formed, it is expected to revert to the previous intermediate and finally enter the correct reaction path. It also seems that the same effect is responsible for the observed *(R)*-stereoselectivity of the reaction. The binding of fumarate in the pro-*(S)* position results in an inverse preference of regioselectivity (controlled by TS2), leading to a preferential attack of the benzyl radical on the proximal C2 carbon atom. However, this pathway is associated with a very high barrier of radical quenching, effectively excluding the pathway leading to *(S)*-benzylsuccinate.

Occurrence of BSS and Other FAEs in Diverse Anaerobic Bacteria

In the case of anaerobic degradation of toluene and other methyl-substituted aromatic hydrocarbons, an initial attack via fumarate addition is the only known mechanism known so far with the exception of a recently described methyl group hydroxylation of *p*-cymene by a molybdenum-containing hydroxylase [Strijkstra et al., 2014]. Anaerobic toluene degraders are known to occur in many physiological groups of microorganisms, especially denitrifying bacteria, metal ion and sulfate-reducing species, a phototropic [Zengler et al., 1999] and several syntrophic proton-reducing bacterial species in methanogenic cocultures that are often affiliated with the genus *Desulfosporosinus* [Cupples, 2011; Fowler et al.,

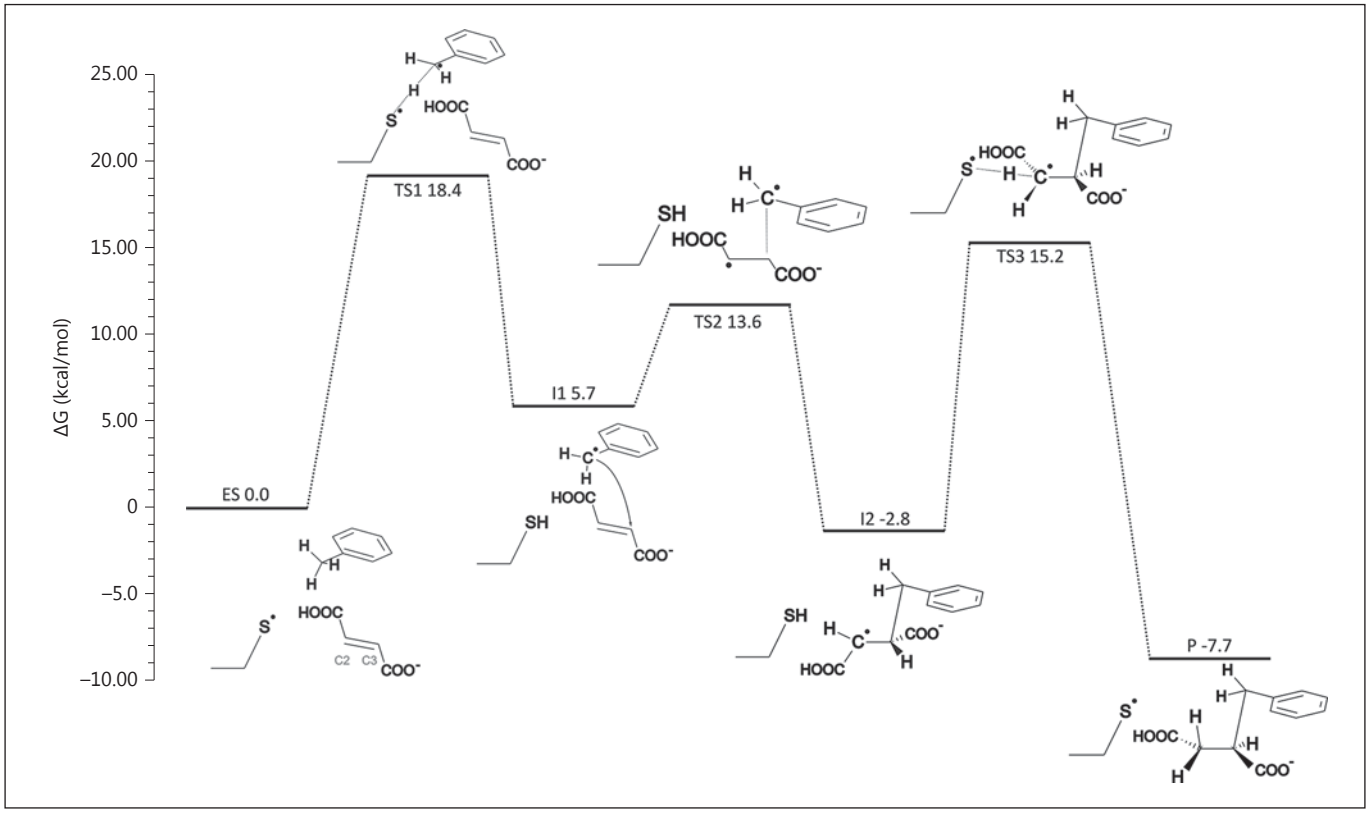

Fig. 4. DFT model of the reaction mechanism of BSS. Calculations were started with the enzyme containing both bound substrates in the active site and already carrying a thiyl radical at Cys493 (ES state). The calculated energy values for the various transition states and intermediates are shown for the respective partial reactions of the most plausible of several studied alternative pathways. Note that the dots shown in the transition states represent the partial radical character of the respective atoms, whereas those in the intermediate states have be attributed to (almost) full radical properties of the indicated atoms.

2014]. Most of the known toluene-degrading denitrifying bacteria belong to the genera *Thauera*, *Azoarcus*, *Georgfuchsia* and *Aromatoleum* within the betaproteobacterial family *Rhodocyclaceae* (fig. 5; β-NRB, nitrate-reducing bacteria), while additional unrelated denitrifying strains affiliated to the genera *Magnetospirillum (*Alphaproteobacteria*)* and *Herminiimonas* (Betaproteobacteria) have apparently acquired this property via lateral gene transfer from members of the former group (fig. 5; αβ-NRB). The metal ion-reducing species reduce either Fe^{III} to Fe^{II}, Mn^{IV} to Mn^{II} or U^{VI} to U^{IV} and belong mostly to the strictly anaerobic genera *Geobacter (*Deltaproteobacteria*)* or *Georgfuchsia* (Betaproteobacteria). Many species of toluene-degrading sulfate-reducing bacteria are known, which affiliate mostly with the genera *Desulfobacula*, *Desulfobulbus* or *Desulfosarcina* [Abu Laban et al., 2015; Harms et al., 1999a, b; Kleindienst et al., 2014; Rabus et al., 1993; Wöhlbrand et al., 2013] within the Deltaproteobacteria and with the genera *Desulfotomaculum* or *Desulfosporosinus* within the Firmicutes [Morasch et al., 2004; Pester et al., 2012]. These species are usually restricted to the degradation of toluene and a few close analogs, such as halogenated toluenes and the cresol or xylene isomers, which can be converted to the succinate adducts by the same BSS isoenzyme as toluene [Beller and Spormann, 1999; Müller et al., 1999, 2001; Verfürth et al., 2004]. Based on the sequences of the large subunits, the BSS orthologs from all these strains clearly form a monophyletic clade in a phylogenetic tree (fig. 5). The branching order is mainly dependent on the phylogenetic affiliation, except for some cases of lateral gene transfer (e.g. from a strain of the *Rhodocyclaceae* to the unrelated genera *Magnetobacterium* or *Herminiimonas*). Two homology clusters of BSS can be observed within the sulfate-reducing bacteria, one (SRB1 in fig. 5) containing the sequences from Deltaproteobacteria (including the Fe^{III}-reducing

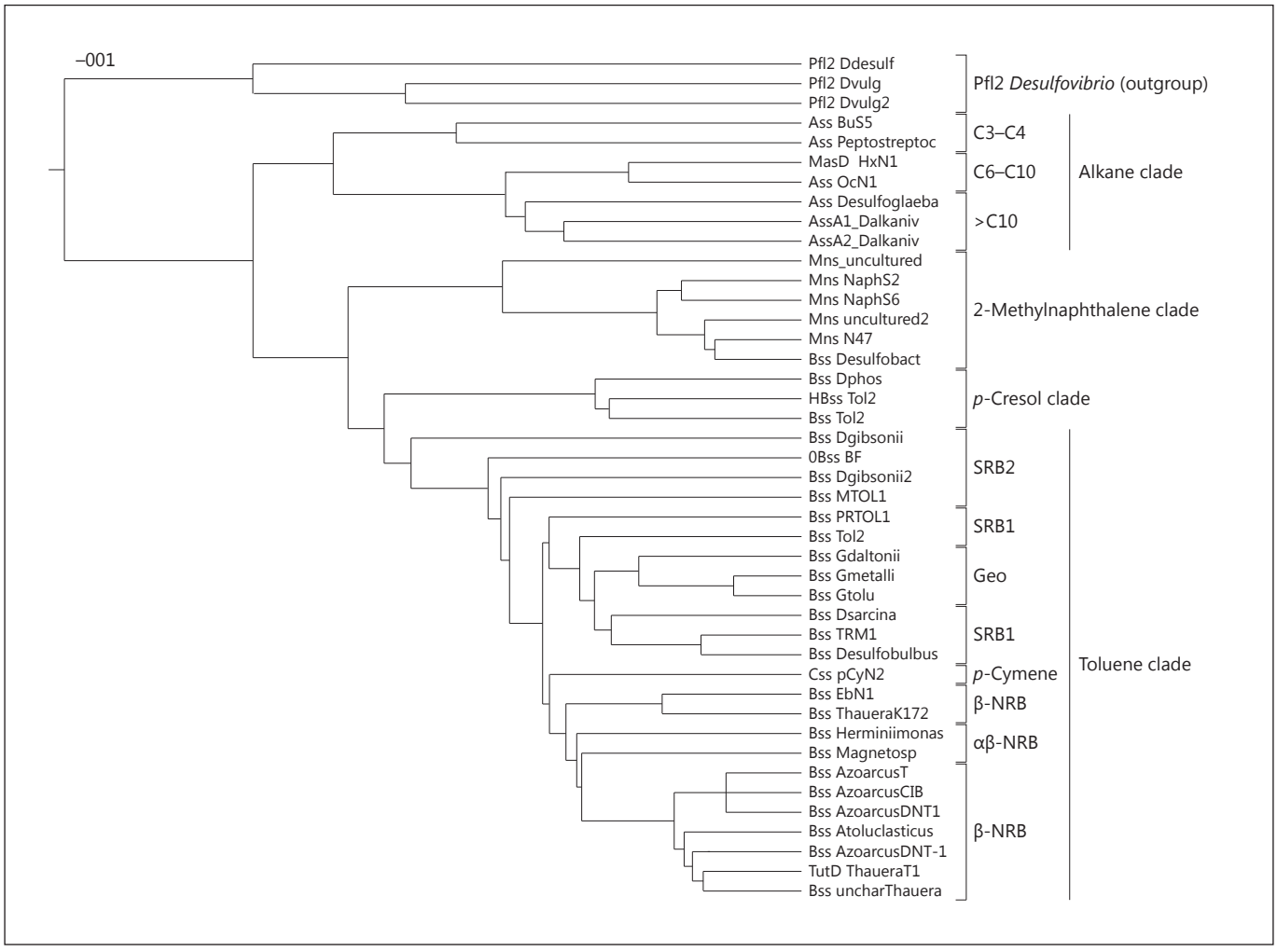

Fig. 5. Phylogenetic tree of FAEs. The tree was constructed by multiple alignment of the sequences of the large subunits of FAEs using the ClustalW2 program available on the EMBL-EBI website. SRB1 and SRB2 = Sulfate-reducing bacteria affiliated to the Deltaproteobacteria or the Firmicutes, respectively; Geo = *Geobacter* strains. All sequences of the non-BSS clade enzymes are from sulfate-reducing bacteria. Initial sequences of alkane-, 2-methylnaphthalene-, *p*-cresol- and *p*-cymene-converting FAEs were reported in Grundmann et al. [2008], Selesi et al. [2009], Wöhlbrand et al. [2013] and Strijkstra et al. [2014], respectively. As the outgroup, a number of similar uncharacterized GREs from *Desulfovibrio* strains have been used, which belong to the 'Pfl2' group of GREs but are certainly not members of the FAE group (based on missing active-site residue homologs, such as the universally conserved Arg508 or the amino acids surrounding Cys493, and the lack of genes for small subunits in their respective operons).

Geobacter species) and the other those from Gram-positive strains (SRB2 in fig. 5). Remarkably, the single known sequence of a *p*-cymene-activating FAE from strain *p*CyN2 [Strijkstra et al., 2014], which is closely affiliated with *Thauera terpenica* [Heider and Fuchs, 2005], is located just between the branches representing the BSS orthologs of nitrate- and sulfate-reducing species (fig. 5).

Three additional subfamilies of paralogous FAE isoenzymes catalyzing fumarate addition to various aromatic or aliphatic compounds other than toluene were recently identified in diverse bacteria: the sulfate-reducing species *Desulfobacula toluolica* contains a second operon coding for an FAE specific for *p*-cresol activation next to the normal *bss* operon involved in toluene metabolism [Wöhlbrand et al., 2013]. The derived sequence of the large subunit indeed forms a separate cluster in the phylogenetic tree together with the sequences of some closely related uncharacterized FAEs, which may therefore be tentatively assigned as *p*-cresol-specific *p*-hydroxybenzylsuccinate synthases (HBSS; fig. 5). Moreover, FAEs have been im-

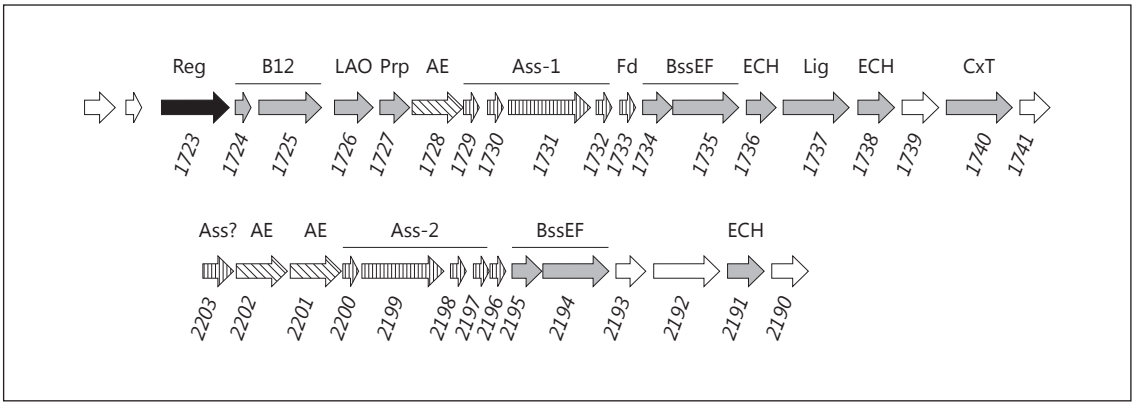

Fig. 6. Organization of two *ass* operons identified in the genome sequence of the alkane-degrading *Desulfatibacillum alkenivorans*. The numbers refer to those assigned to the respective genes during the sequencing project (e.g. Dalk_1723). The functionalities of the enzymes encoded in either apparent operon for alkane metabolism have not completely settled [Callaghan et al., 2012]. Reg = Regulator; B12 = coenzyme B_{12}-dependent mutase; LAO = fatty acid transport system; PrpD = methylcitrate dehydratase; AE = activating enzyme; Ass = alkylsuccinate synthase (including putative additional small subunits); Fd = ferredoxin; BssEF = BssEF-like accessory proteins; ECH = enoyl-CoA hydratase; Lig = CoA ligase; CxT = carboxytransferase.

plicated in several naphthalene and 2-methylnaphthalene-degrading sulfate-reducing isolates and enrichment cultures to effect 2-methylnaphthalene activation, generating a 2-(2-methylnaphthyl)succinate intermediate [Galushko et al., 1999; Musat et al., 2009; Selesi et al., 2009]. Phylogenetic analysis with the sequences of the respective large subunits of these enzymes (2-(2-methylnaphthalene)succinate synthase, MNS) indeed indicates that they form another homology cluster, representing a distinct MNS clade with less sequence conservation to the BSS and HBSS paralogs (fig. 5). Finally, alkane-degrading species of nitrate- or sulfate- reducing bacteria have been shown to use a special clade of FAE (labeled alkanesuccinate synthase, ASS) even for the initial step of alkane activation, forming branched alkylsuccinate adducts at the subterminal methylene group of the alkane [Callaghan et al., 2008, 2010; Grundmann et al., 2008; Rabus et al., 2001].

The sequences of alkane-activating FAEs appear to differ mostly relative to the chain lengths of their respective substrates: three subgroups can be seen, which correspond to the enzymes activating very short-chain alkanes like propane or butane [Jaekel et al., 2013; Kniemeyer et al., 2007; Musat, 2015], medium-chain alkanes like hexane or octane [Grundmann et al., 2008; Rabus et al., 2001; Zedelius et al., 2011] or long-chain alkanes of more than 10 C-atoms [Callaghan, 2013a, b]. Among these enzymes, propane activation appears to be exceptional in adding the fumarate either to the secondary methylene carbon or to one of the primary methyl groups of propane [Kniemeyer et al., 2007], while all other alkanes are activated exclusively at their subterminal methylene groups. Anaerobic alkane degraders are known within the denitrifying *Rhodocyclaceae* (e.g. *Aromatoleum* strain HxN1), as well as among the sulfate-reducing bacteria (e.g. the genera *Desulfatibacillum* or *Desulfoglaeba*). Participation of these FAEs in anaerobic alkane metabolism has been clearly demonstrated based on metabolite analysis, genome and metagenome sequencing, proteomic studies and the presence of the typical glycyl radical EPR signal in cells grown on alkanes [Callaghan, 2013a, b; Grundmann et al., 2008; Rabus et al., 2001]. The outline of the further degradative pathway of the branched succinate adducts formed during alkane activation has been studied for the hexane-degrading denitrifying strain HxN1. This pathway involves activation of the (1-methylalkyl)succinate intermediate to a CoA thioester, followed by rearrangement of the carbon skeleton in a reaction reminiscent of that of methylmalonyl-CoA mutase and then decarboxylation and β-oxidation, leading ultimately to three acetyl-CoA and one propionyl-CoA [Wilkes et al., 2002]. No biochemical characterization has been reported for any alkane-activating FAE, but it appears from the available sequences of the corresponding operons that alkane-activating FAEs may contain at least one additional Fe-S cluster-containing small subunit in comparison to BSS or the other FAEs (fig. 6). In addition to genes coding for paralogs of the activating enzymes

and the α-, β- and γ-subunits, the known operons usually contain additional genes coding for highly conserved small proteins that exhibit the characteristic Cys-rich sequence motives for ligating the unusual type of Fe_4S_4 clusters observed in the β- and γ-subunits of BSS [Grundmann et al., 2008, Callaghan et al., 2013a, b] (fig. 6). Moreover, the apparent *ass-1* operon of *D. alkenivorans* carries additional genes, which probably code for enzymes of the further degradation pathway, such as a CoA ligase, a coenzyme B_{12}-containing mutase unrelated to any member of the known mutase subfamilies [Ebenau-Jehle et al., 2012], which is probably involved in rearranging the activated alkylsuccinate intermediate, a transcarboxylase and several enzymes of a β-oxidation pathway (fig. 6).

Finally, an FAE has also been reported to be involved in an ethylbenzene-degrading sulfate-reducing bacterium initiating a degradation pathway whereby fumarate adds to the methylene group of ethylbenzene [Kniemeyer et al., 2003], and even cyclic alkanes like cyclohexane are apparently degraded via fumarate addition [Musat et al., 2009; Jaekel et al., 2015]. However, no sequence information is available so far for the corresponding enzymes. A recent study even reported anaerobic alkane degradation by the thermophilic sulfate-reducing archaeal species *Archaeoglobus fulgidus*, but the GRE sequence pointed out by the authors as a potential catalyst for the initial reaction does not show any resemblance to other FAEs and rather appears to belong to the family of uncharacterized Pfl2-like proteins, leaving an open question concerning the potential pathway [Khelifi et al., 2014].

Structural Comparison of BSS and FAE Paralogs

Table 1 shows the conservedness of side chains lining the predicted active site cavity of BSS from sequence (fig. 5) and structural alignments of the various known FAEs. Predicted active site geometries of HBSS, MNS and ASS were compared with those of BSS based on homology models derived from the crystal structure of BSS (fig. 7). The homology protein models for HBSS, MNS and ASS were calculated using Maestro version 10.0 from the Schrödinger package (Schrödinger, New York, N.Y., USA). Model building was performed using the amino acid sequences of the large subunits of HBSS from *D. toluolica* [Wöhlbrand et al., 2013], MNS from strain NaphS6 [Musat et al., 2009] and alkylsuccinate synthase-1 (ASS) from *D. alkenivorans* (see table 1 for accession No.) [Callaghan et al., 2008]. All FAEs displayed a universal conservation of the catalytic thiol/thiyl moiety (Cys493 in BSS) and the Arg508 (BSS numbering) involved in fumarate binding, demonstrating the eminently important roles of these amino acids for catalysis. While Cys493 is obviously conserved in all known GREs, the presence of a conserved Arg at a position corresponding to Arg508 may be taken as a first indication for functionality as a potential FAE (e.g. the three outgroup sequences in fig. 5 contain a Glu at this position). Another universally conserved amino acid is Val709, whereas all the other active site amino acids shown in table 1 may be changed in at least a few members of the FAE. For example, the Met directly following the active site Cys is almost universally conserved, but is exchanged to Ile in the sequences of the short alkane-activating ASS paralogs.

HBSS displayed a rather high amino acid sequence identity with BSS (49%) and contains only one different side chain in the active site, a phenylalanine instead of tyrosine (table 1; fig. 7a). MNS showed 45% amino acid sequence identity to BSS and again displays only one different side chain in the active site, a glutamine instead of a phenylalanine (table 1; fig. 7b). Finally, ASS exhibited a quite low overall amino acid sequence identity with BSS (33%) and deviated most from the sequence of BSS, exhibiting 8 amino acid changes in the 13 positions predicted to constitute the active site (table 1). One of the most significant differences between ASS and all other sequences of FAEs seems to be the presence of a Gln-Ala motif instead of an otherwise conserved Val-Leu immediately preceding the catalytic Cys (Cys493 in BSS). It is

Table 1. Conserved amino acids in the active sites among FAE paralogs

BSS (PDB codes 4pkc, 4pkf)	HBSS (homology protein model)	MNS (homology protein model)	ASS (homology protein model)
Tyr197	Phe161	Tyr172	Tyr189
Ser199	Ser163	Ser174	Gly191
Ser328	Ser292	Ser309	Gly317
Phe385	Phe349	Gln366	Leu372
Leu391	Leu355	Leu372	Thr378
Val491	Val448	Val465	Gln471
Leu492	Leu449	Leu466	Ala472
Cys493	Cys450	Cys467	Cys473
Met494	Met451	Met468	Met474
Arg508	Arg465	Arg482	Arg488
Gly512–Gly513	Gly469-Ser470	Gly486–Gly487	Ala492-Thr493
Asn615	Asn572	Asn589	Thr594
Val709	Val666	Val682	Val688

Accession No.: WP_014956012 for HBSS, CAO72222 for MNS and ABH11460 for ASS.

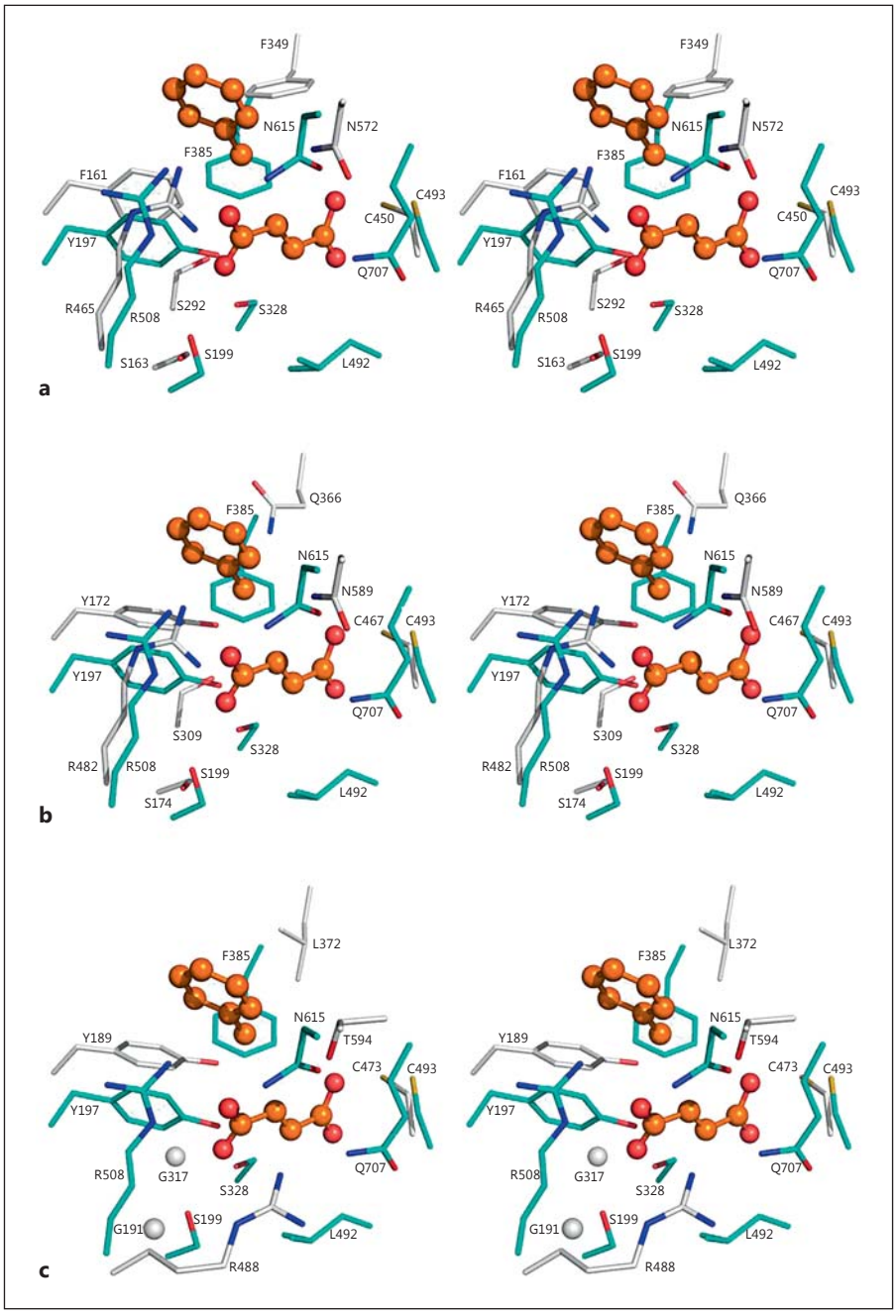

Fig. 7. Substrate-binding site models of FAEs. Stereo-views of the active site pocket of BSS (PDB code 4pkf) after MD/MM relaxation to accommodate binding of the substrates [Szaleniec et al., submitted] compared with those of HBSS (**a**), MNS (**b**) and ASS (**c**). Amino acid side chains are shown in stick mode. The color code for BSS is cyan (carbon), red (oxygen), blue (nitrogen) and yellow (sulfur). The overlaying homology protein models use grey for carbon. The binding mode for the substrates fumarate and toluene calculated for BSS from *T. aromatica* strain T1 is shown in ball-and-stick mode (orange for carbon and red for oxygen) to help visualize the void volumes of the respective active site pockets.

obvious that the more related structural models of HBSS and MNS show a very similar positioning of the key residues analogous to Cys493 and Arg508 of BSS as well as several other active site amino acids, suggesting very similar functions in fumarate binding. Several other amino acids deviate in their positions, which may indicate some flexibility and repositioning during substrate binding. In the case of MNS, the most obvious amino acid exchange (Phe385 of BSS to Gln366) results in the loss of a phenyl ring, which may indeed allow the enzyme to accommodate the two-ring structure of 2-methylnaphthalene in the opened space (fig. 7b). The different side-chain composition observed in ASS with many exchanges of larger to smaller amino acids might allow a bigger void volume for the active site pocket in ASS compared to BSS, which may be better suited to accommodate large alkanes (fig.

7c). However, the last structure model of ASS, in particular, has to be regarded with caution because of the low primary sequence similarity with BSS. A noticeable problematic feature in the predicted model is, for example, the apparent severe misalignment of the conserved Arg residue (Arg488 in ASS) with the docked fumarate cosubstrate in BSS-like conformation (fig. 7c), which probably arises from the limitations of correctly predicting the enzyme structure. Alternatively, the fumarate may be bound in a quite different angle in the active site of ASS compared to BSS to facilitate its attack at the subterminal methylene group of alkanes. The final evaluation of the side-chain geometries and the amino acids relevant for substrate binding and discrimination among BSS, HBSS, MNS and ASS must await more detailed biochemical and structural characterization.

Note Added in Proof

While this manuscript was under review, a new report was published which delivered structures of BSS with bound substrates [Funk et al., 2015]. The reported structures are at a resolution of 3.3 and 2.0 Å for BSS containing both fumarate and toluene or fumarate only, respectively, and allow the fumarate binding mode to be clearly identified. These results confirm the strong anchoring of one carboxylic group via ionic interactions to Arg508 while the other carboxylic group forms H bonds to main-chain atoms of the Cys493 loop. Moreover, a pro-*(R)* position of the bound fumarate was also confirmed. Unfortunately, the position of bound toluene seems to remain largely speculative due to the low electron density in the active site of the available crystals. Therefore, the results of our modeling studies are fully consistent with these new experimental data.

Acknowledgments

J. Heider, B.M. Martins, W. Buckel and B.T. Golding acknowledge the financial support from the Deutsche Forschungsgemeinschaft (Priority Programme 1319), and additional funding by the state of Hessen (via the LOEWE center for synthetic microbiology to J.H. and W.B.) or by the European Commission (via COST action CM1201, biomimetic radical chemistry, to B.T.G.). M. Szaleniec acknowledges the financial support from Polish computational grants MNiSW/SGI4700/PAN/038/2007 and MNiSW/IBM_BC_HS21/PAN/038/200 and from the Marian Smoluchowski Krakow Research Consortium.

References

Abu Laban N, Tan B, Dao A, Foght J: Draft genome sequence of uncultivated toluene-degrading *Desulfobulbaceae* bacterium Tol-SR, obtained by stable isotope probing using [$^{13}C_6$]toluene. Genome Announc 2015; 3:e01423.

Achong GR, Rodriguez AM, Spormann AM: Benzylsuccinate synthase of *Azoarcus sp.* strain T: cloning, sequencing, transcriptional organization, and its role in anaerobic toluene and *m*-xylene mineralization. J Bacteriol 2001; 183:6763–6770.

Aeckersberg F, Bak F, Widdel F: Anaerobic oxidation of saturated hydrocarbons to CO_2 by a new type of sulfate-reducing bacterium. Arch Microbiol 1991;156:5–14.

Aklujkar M, Krushkal J, DiBartolo G, Lapidus A, Land ML, Lovley DR: The genome sequence of *Geobacter metallireducens*: features of metabolism, physiology and regulation common and dissimilar to *Geobacter sulfurreducens*. BMC Microbiol 2009;9:109.

Altenschmidt U, Fuchs G: Anaerobic degradation of toluene in denitrifying *Pseudomonas* sp.: indication for toluene methylhydroxylation and benzoyl-CoA as central aromatic intermediate. Arch Microbiol 1991;156:152–158.

Beller HR, Reinhard M, Grbić-Galić D: Metabolic by-products of anaerobic toluene degradation by sulfate-reducing enrichment cultures. Appl Environ Microbiol 1992;58:3192–3195.

Beller HR, Spormann AM: Benzylsuccinate formation as a means of anaerobic toluene activation by sulfate-reducing strain PRTOL1. Appl Environ Microbiol 1997a;63:3729–3731.

Beller HR, Spormann AM: Anaerobic activation of toluene and *o*-xylene by addition to fumarate in denitrifying strain T. J Bacteriol 1997b;179:670–676.

Beller HR, Spormann AM: Analysis of the novel benzylsuccinate synthase reaction for anaerobic toluene activation based on structural studies of the product. J Bacteriol 1998;180: 5454–5457.

Beller HR, Spormann AM: Substrate range of benzylsuccinate synthase from *Azoarcus* sp. Strain T. FEMS Microbiol Lett 1999;178:147–153.

Bharadwaj VS, Dean AM, Maupin CM: Insights into the glycyl radical enzyme active site of benzylsuccinate synthase: a computational study. J Am Chem Soc 2013;135:12279–12288.

Biegert T, Fuchs G, Heider J: Evidence that anaerobic oxidation of toluene in the denitrifying bacterium *Thauera aromatica* is initiated by formation of benzylsuccinate from toluene and fumarate. Eur J Biochem 1996;238:661–668.

Booker SJ: Anaerobic functionalization of unactivated C-H bonds. Curr Opin Biotechnol 2011;22:406–414.

Bozinovski D, Taubert M, Kleinsteuber S, Richnow H-H, von Bergen M, Vogt C, Seifert J: Metaproteogenomic analysis of a sulfate-reducing enrichment culture reveals genomic organization of key enzymes in the *m*-xylene degradation pathway and metabolic activity of proteobacteria. Syst Appl Microbiol 2014; 37:488–501.

Buckel W, Golding BT: Radical enzymes in anaerobes. Annu Rev Microbiol 2006;60:27–49.

Butler JE, He Q, Nevin KP, He Z, Zhou J, Lovley DR: Genomic and microarray analysis of aromatics degradation in *Geobacter metallireducens* and comparison to a *Geobacter* isolate from a contaminated field site. BMC Genomics 2007;8:180.

Callaghan AV: Metabolomic investigations of anaerobic hydrocarbon-impacted environments. Curr Opin Biotechnol 2013a;24:506–515.

Callaghan AV: Enzymes involved in the anaerobic oxidation of n-alkanes: from methane to long-chain paraffins. Front Microbiol 2013b;4:89.

Callaghan AV, Davidova IA, Savage-Ashlock K, Parisi VA, Gieg LM, Suflita JM, Kukor JJ, Wawrik B: Diversity of benzyl- and alkylsuccinate synthase genes in hydrocarbon-impacted environments and enrichment cultures. Environ Sci Technol 2010;44:7287–7294.

Callaghan AV, Gieg LM, Kropp KG, Suflita JM, Young LY: Comparison of mechanisms of alkane metabolism under sulfate-reducing conditions among two bacterial isolates and a bacterial consortium. Appl Environ Microbiol 2006;72:4274–4282.

Callaghan AV, Morris BEL, Pereira IAC, McInerney MJ, Austin RN, Groves JT, Kukor JJ, Suflita JM, Young LY, Zylstra GJ, Wawrik B: The genome sequence of *Desulfatibacillum alkenivorans* AK-01: a blueprint for anaerobic alkane oxidation. Environ Microbiol 2012;14:101–113.

Callaghan AV, Wawrik B, Ní Chadhain SMM, Young LY, Zylstra GJ: Anaerobic alkane-degrading strain AK-01 contains two alkylsuccinate synthase genes. Biochem Biophys Res Commun 2008;366:142–148.

Coschigano PW: Transcriptional analysis of the *tutE tutFDGH* gene cluster from *Thauera aromatica* strain T1. Appl Environ Microbiol 2000;66:1147–1151.

Coschigano PW, Wehrman TS, Young LY: Identification and analysis of genes involved in anaerobic toluene metabolism by strain T1: putative role of a glycine free radical. Appl Environ Microbiol 1998;64:1650–1656.

Coschigano PW, Young LY: Identification and sequence analysis of two regulatory genes involved in anaerobic toluene metabolism by strain T1. Appl Environ Microbiol 1997;63:652–660.

Craciun S, Balskus EP: Microbial conversion of choline to trimethylamine requires a glycyl radical enzyme. Proc Natl Acad Sci USA 2012;109:21307–21312.

Craciun S, Marks JA, Balskus EP: Characterization of choline trimethylamine-lyase expands the chemistry of glycyl radical enzymes. ACS Chem Biol 2014;9:1408–1413.

Cupples AM: The use of nucleic acid based stable isotope probing to identify the microorganisms responsible for anaerobic benzene and toluene biodegradation. J Microbiol Meth 2011;85:83–91.

Dolfing J, Zeyer J, Binder-Eicher P: Isolation and characterization of a bacterium that mineralizes toluene in the absence of molecular oxygen. Arch Microbiol 1990;154:336–341.

Duboc-Toia C, Hassan AK, Mulliez E, Ollagnier-de Choudens S, Fontecave M, Leutwein C, Heider J: Very high-field EPR study of glycyl radical enzymes. J Am Chem Soc 2003;125:38–39.

Ebenau-Jehle C, Thomas M, Scharf G, Kockelkorn D, Knapp B, Schühle K, Heider J, Fuchs G: Anaerobic metabolism of indoleacetate. J Bacteriol 2012;194:2894–2903.

Eklund H, Fontecave M: Glycyl radical enzymes: a conservative structural basis for radicals. Structure 1999;7:R257–R262.

Evans PJ, Ling W, Goldschmidt B, Ritter ER, Young LY: Metabolites formed during anaerobic transformation of toluene and *o*-xylene and their proposed relationship to the initial steps of toluene mineralization. Appl Environ Microbiol 1992;58:496–501.

Foght J: Anaerobic biodegradation of aromatic hydrocarbons: pathways and prospects. J Mol Microbiol Biotechnol 2008;15:93–120.

Fowler SJ, Gutierrez-Zamora M-LL, Manefield M, Gieg LM: Identification of toluene degraders in a methanogenic enrichment culture. FEMS Microbiol Ecol 2014;89:625–636.

Frazer AC, Coschigano PW, Young LY: Toluene metabolism under anaerobic conditions: a review. Anaerobe 1995;1:293–303.

Fuchs G, Boll M, Heider J: Microbial degradation of aromatic compounds – from one strategy to four. Nat Rev Microbiol 2011;9:803–816.

Funk MA, Judd ET, Marsh EN, Elliott SJ, Drennan CL: Structures of benzylsuccinate synthase elucidate roles of accessory subunits in glycyl radical enzyme activation and activity. Proc Natl Acad Sci USA 2014;111:10161–10166.

Funk MA, Marsh EN, Drennan CL: Substrate-bound structures of benzylsuccinate synthase reveal how toluene is activated in anaerobic hydrocarbon degradation. J Biol Chem 2015;290:22398–22408.

Galushko AS, Minz D, Schink B, Widdel F: Anaerobic degradation of naphthalene by a pure culture of a novel type of marine sulphate-reducing bacterium. Environ Microbiol 1999;5:415–420.

Grundmann O, Behrends A, Rabus R, Amann J, Halder T, Heider J, Widdel F: Genes encoding the candidate enzyme for anaerobic activation of *n*-alkanes in the denitrifying bacterium strain HxN1. Environ Microbiol 2008;10:376–385.

Harms G, Rabus R, Widdel F: Anaerobic oxidation of the aromatic plant hydrocarbon *p*-cymene by newly isolated denitrifying bacteria. Arch Microbiol 1999a;172:303–312.

Harms G, Zengler K, Rabus R: Anaerobic oxidation of *o*-xylene, *m*-xylene, and homologous alkylbenzenes by new types of sulfate-reducing bacteria. Appl Environ Microbiol 1999b;65:999–1004.

Heider J: Adding handles to unhandy substrates: anaerobic hydrocarbon activation mechanisms. Curr Opin Chem Biol 2007;11:188–194.

Heider J, Fuchs G: Genus Thauera; in Brenner DJ, Krieg NR, Staley JT, Garrity GM (eds): Bergey's Manual of Systematic Bacteriology, ed 2. Berlin, Springer, 2005, vol 2C, pp 907–913.

Heider J, Rabus R: Genomic insights in the anaerobic biodegradation of organic pollutants; in Diaz E (ed): Microbial Biodegradation. Genomics and Molecular Biology. Norfolk, Caister, 2008, pp 25–54.

Heider J, Schühle K: Anaerobic biodegradation of hydrocarbons including methane; in Rosenberg E, DeLong EF, Thompson F, Lory S, Stackebrandt E (eds): The Prokaryotes: Prokaryotic Physiology and Biochemistry. New York, Springer, 2013, pp 601–630.

Heider J, Spormann AM, Beller HR, Widdel F: Anaerobic bacterial metabolism of hydrocarbons. FEMS Microbiol Rev 1998;22:459–473.

Hermuth K, Leuthner B, Heider J: Operon structure and expression of the genes for benzylsuccinate synthase in *Thauera aromatica* strain K172. Arch Microbiol 2002;177:132–138.

Hilberg M, Pierik AJ, Eckhard B, Lippert ML, Heider J: Identification of FeS clusters in the glycyl-radical enzyme benzylsuccinate synthase via EPR and Mössbauer spectroscopy. J Biol Inorg Chem 2011;17:49–56.

Himo F: Catalytic mechanism of benzylsuccinate synthase, a theoretical study. J Phys Chem B 2002;106:7688–7692.

Himo F: C-C bond formation and cleavage in radical enzymes, a theoretical perspective. Biochim Biophys Acta 2005;1707:24–33.

Jaekel U, Musat N, Adam B, Kuypers M, Grundmann O, Musat F: Anaerobic degradation of propane and butane by sulfate-reducing bacteria enriched from marine hydrocarbon cold seeps. ISME J 2013;7:885–895.

Jaekel U, Zedelius J, Wilkes H, Musat F: Anaerobic degradation of cyclohexane by sulfate-reducing bacteria from hydrocarbon-contaminated marine sediments. Front Microbiol 2015;6:116.

Jarling R, Sadeghi M, Drozdowska M, Lahme S, Buckel W, Rabus R, Widdel F, Golding BT, Wilkes H: Stereochemical investigations reveal the mechanism of the bacterial activation of *n*-alkanes without oxygen. Angew Chem Int Ed Engl 2012;51:1334–1338.

Juárez JF, Zamarro MTT, Eberlein C, Boll M, Carmona M, Díaz E: Characterization of the *mbd* cluster encoding the anaerobic 3-methylbenzoyl-CoA central pathway. Environ Microbiol 2013;15:148–166.

Khelifi N, Ali OA, Roche P, Grossi V: Anaerobic oxidation of long-chain *n*-alkanes by the hyperthermophilic sulfate-reducing archaeon, *Archaeoglobus fulgidus*. ISME J 2014;8:2153–2166.

Kleindienst S, Herbst FA, Stagars M, von Netzer F, Von Bergen M, Seifert J, Peplies J, Amann R, Musat F, Lueders T, Knittel K: Diverse sulfate-reducing bacteria of the D*esulfosarcina/Desulfococcus* clade are the key alkane degraders at marine seeps. ISME J 2014;8:2029–2044.

Knappe J, Sawers G: A radical-chemical route to acetyl-CoA: the anaerobically induced pyruvate formate-lyase system of *Escherichia coli*. FEMS Microbiol Rev 1990;6:383–398.

Kniemeyer O, Fischer T, Wilkes H: Anaerobic degradation of ethylbenzene by a new type of marine sulfate-reducing bacterium. Appl Environ Microbiol 2003;69:760–768.

Kniemeyer O, Musat F, Sievert SM, Knittel K, Wilkes H, Blumenberg M, Michaelis W, Classen A, Bolm C, Joye SB, Widdel F: Anaerobic oxidation of short-chain hydrocarbons by marine sulphate-reducing bacteria. Nature 2007;449:898–901.

Krieger CJ, Beller HR, Reinhard M, Spormann AM: Initial reactions in anaerobic oxidation of *m*-xylene by the denitrifying bacterium *Azoarcus sp.* strain T. J Bacteriol 1999;181:6403–6410.

Krieger CJ, Roseboom W, Albracht SP, Spormann AM: A stable organic free radical in anaerobic benzylsuccinate synthase of *Azoarcus sp.* strain T. J Biol Chem 2001;276:12924–12927.

Kube M, Heider J, Amann J, Hufnagel P, Kühner S, Beck A, Reinhardt R, Rabus R: Genes involved in the anaerobic degradation of toluene in a denitrifying bacterium, strain EbN1. Arch Microbiol 2004;181:182–194.

Kühner S, Wöhlbrand L, Fritz I, Wruck W, Hultschig C, Hufnagel P, Kube M, Reinhardt R, Rabus R: Substrate-dependent regulation of anaerobic degradation pathways for toluene and ethylbenzene in a denitrifying bacterium, strain EbN1. J Bacteriol 2005;187:1493–1503.

Leuthner B, Heider J: A two-component system involved in regulation of anaerobic toluene metabolism in *Thauera aromatica*. FEMS Microbiol Lett 1998;166:35–41.

Leuthner B, Heider J: Anaerobic toluene catabolism of *Thauera aromatica*: the *bbs* operon codes for enzymes of beta oxidation of the intermediate benzylsuccinate. J Bacteriol 2000;182:272–277.

Leuthner B, Leutwein C, Schulz H, Hörth P, Haehnel W, Schiltz E, Schägger H, Heider J: Biochemical and genetic characterization of benzylsuccinate synthase from *Thauera aromatica*: a new glycyl radical enzyme catalysing the first step in anaerobic toluene metabolism. Mol Microbiol 1998;28:615–628.

Leutwein C, Heider J: Anaerobic toluene-catabolic pathway in denitrifying *Thauera aromatica*: activation and β-oxidation of the first intermediate, *(R)*-(+)-benzylsuccinate. Microbiology 1999;145:3265–3271.

Leutwein C, Heider J: Succinyl-CoA:*(R)*-benzylsuccinate CoA-transferase: an enzyme of the anaerobic toluene catabolic pathway in denitrifying bacteria. J Bacteriol 2001;183:4288–4295.

Leutwein C, Heider J: *(R)*-benzylsuccinyl-CoA dehydrogenase of *Thauera aromatica*, an enzyme of the anaerobic toluene catabolic pathway. Arch Microbiol 2002;178:517–524.

Li L, Marsh EN: Deuterium isotope effects in the unusual addition of toluene to fumarate catalyzed by benzylsuccinate synthase. Biochemistry 2006a;45:13932–13938.

Li L, Marsh EN: Mechanism of benzylsuccinate synthase probed by substrate and isotope exchange. J Am Chem Soc 2006b;128:16056–16057.

Li L, Marsh EN: Subunit structure of benzylsuccinate synthase. Biochemistry 2009;48:1284–1292.

Martins BM, Blaser M, Feliks M, Ullmann GM, Buckel W, Selmer T: Structural basis for a Kolbe-type decarboxylation catalyzed by a glycyl radical enzyme. J Am Chem Soc 2011;133:14666–14674.

Mechichi T, Stackebrandt E, Gad'on N, Fuchs G: Phylogenetic and metabolic diversity of bacteria degrading aromatic compounds under denitrifying conditions, and description of *Thauera phenylacetica* sp. nov., *Thauera aminoaromatica* sp. nov., and *Azoarcus buckelii* sp. nov. Arch Microbiol 2002;178:26–35.

Morasch B, Schink B, Tebbe CC, Meckenstock RU: Degradation of *o*-xylene and *m*-xylene by a novel sulfate-reducer belonging to the genus *Desulfotomaculum*. Arch Microbiol 2004;181:407–417.

Müller JA, Galushko AS, Kappler A, Schink B: Anaerobic degradation of *m*-cresol by *Desulfobacterium cetonicum* is initiated by formation of 3-hydroxybenzylsuccinate. Arch Microbiol 1999;172:287–294.

Müller JA, Galushko AS, Kappler A, Schink B: Initiation of anaerobic degradation of *p*-cresol by formation of 4-hydroxybenzylsuccinate in *Desulfobacterium cetonicum*. J Bacteriol 2001;183:752–757.

Musat F: The anaerobic degradation of gaseous, nonmethane alkanes – from in situ processes to microorganisms. Comput Struct Biotechnol J 2015;13:222–228.

Musat F, Galushko A, Jacob J, Widdel F, Kube M, Reinhardt R, Wilkes H, Schink B, Rabus R: Anaerobic degradation of naphthalene and 2-methylnaphthalene by strains of marine sulfate-reducing bacteria. Environ Microbiol 2009;11:209–219.

O'Brien JR, Raynaud C, Croux C, Girbal L, Soucaille P, Lanzilotta WN: Insight into the mechanism of the B12-independent glycerol dehydratase from *Clostridium butyricum*: preliminary biochemical and structural characterization. Biochemistry 2004;43:4635–4645.

Pester M, Brambilla E, Alazard D, Rattei T, Weinmaier T, Han J, Lucas S, Lapidus A, Cheng J-FF, Goodwin L, Pitluck S, Peters L, Ovchinnikova G, Teshima H, Detter JC, Han CS, Tapia R, Land ML, Hauser L, Kyrpides NC, Ivanova NN, Pagani I, Huntmann M, Wei C-LL, Davenport KW, Daligault H, Chain PS, Chen A, Mavromatis K, Markowitz V, Szeto E, Mikhailova N, Pati A, Wagner M, Woyke T, Ollivier B, Klenk H-PP, Spring S, Loy A: Complete genome sequences of *Desulfosporosinus orientis* DSM765^T, *Desulfosporosinus youngiae* DSM17734^T, *Desulfosporosinus meridiei* DSM13257^T, and *Desulfosporosinus acidiphilus* DSM22704^T. J Bacteriol 2012;194:6300–6301.

Qiao C, Marsh EN: Mechanism of benzylsuccinate synthase: stereochemistry of toluene addition to fumarate and maleate. J Am Chem Soc 2005;127:8608–8609.

Rabus R, Heider J: Initial reactions of anaerobic metabolism of alkylbenzenes in denitrifying and sulfate-reducing bacteria. Arch Microbiol 1998;170:377–384.

Rabus R, Kube M, Heider J, Beck A, Heitmann K, Widdel F, Reinhardt R: The genome sequence of an anaerobic aromatic-degrading denitrifying bacterium, strain EbN1. Arch Microbiol 2005;183:27–36.

Rabus R, Nordhaus R, Ludwig W, Widdel F: Complete oxidation of toluene under strictly anoxic conditions by a new sulfate-reducing bacterium. Appl Environ Microbiol 1993;59:1444–1451.

Rabus R, Trautwein K, Wöhlbrandt L: Towards habitat-oriented systems biology of *'Aromatoleum aromaticum'* EbN1: chemical sensing, catabolic network modulation and growth control in aromatic compound degradation. Appl Microbiol Biotechnol 2014;98:3371–3388.

Rabus R, Widdel F: Conversion studies with substrate analogues of toluene in a sulfate-reducing bacterium, strain Tol2. Arch Microbiol 1995;164:448–451.

Rabus R, Wilkes H, Behrends A, Armstroff A, Fischer T, Pierik AJ, Widdel F: Anaerobic initial reaction of *n*-alkanes in a denitrifying bacterium: evidence for (1-methylpentyl)succinate as initial product and for involvement of an organic radical in *n*-hexane metabolism. J Bacteriol 2001;183:1707–1715.

Raynaud C, Sarçabal P, Meynial-Salles I, Croux C, Soucaille P: Molecular characterization of the 1,3-propanediol (1,3-PD) operon of *Clostridium butyricum*. Proc Natl Acad Sci USA 2003;100:5010–5015.

Reichard P: The evolution of ribonucleotide reduction. Trends Biochem Sci 1997;22:81–85.

Selesi D, Jehmlich N, Bergen Mv, Schmidt F, Rattei T, Tischler P, Lueders T, Meckenstock RU: Combined genomic and proteomic approaches identify gene clusters involved in anaerobic 2-methylnaphthalene degradation in the sulfate-reducing enrichment culture N47. J Bacteriol 2009;192:295–306.

Selmer T, Andrei PI: *p*-Hydroxyphenylacetate decarboxylase from *Clostridium difficile*. A novel glycyl radical enzyme catalysing the formation of *p*-cresol. Eur J Biochem 2001;268:1363–1372.

Selmer T, Pierik AJ, Heider J: New glycyl radical enzymes catalysing key metabolic steps in anaerobic bacteria. Biol Chem 2005;386:981–988.

Seyfried B, Glod G, Schocher R, Tschech A, Zeyer J: Initial reactions in the anaerobic oxidation of toluene and *m*-xylene by denitrifying bacteria. Appl Environ Microbiol 1994;60:4047–4052.

Sofia HJ, Chen G, Hetzler BG, Reyes-Spindola JF, Miller NE: Radical SAM, a novel protein superfamily linking unresolved steps in familiar biosynthetic pathways with radical mechanisms: functional characterization using new analysis and information visualization methods. Nucleic Acids Res 2001;29:1097–1106.

Strijkstra A, Trautwein K, Jarling R, Wöhlbrand L, Dörries M, Reinhardt R, Drozdowska M, Golding BT, Wilkes H, Rabus R: Anaerobic activation of *p*-cymene in denitrifying betaproteobacteria: methyl group hydroxylation versus addition to fumarate. Appl Environ Microbiol 2014;80:7592–7603.

Verfürth K, Pierik AJ, Leutwein C, Zorn S, Heider J: Substrate specificities and electron paramagnetic resonance properties of benzylsuccinate synthases in anaerobic toluene and *m*-xylene metabolism. Arch Microbiol 2004;181:155–162.

Vogel TM, Grbic-Galic D: Incorporation of oxygen from water into toluene and benzene during anaerobic fermentative transformation. Appl Environ Microbiol 1986;52:200–202.

Wilkes H, Rabus R, Fischer T, Armstroff A, Behrends A, Widdel F: Anaerobic degradation of *n*-hexane in a denitrifying bacterium: further degradation of the initial intermediate (1-methylpentyl)succinate via C-skeleton rearrangement. Arch Microbiol 2002;177:235–243.

Wöhlbrand L, Jacob JH, Kube M, Mussmann M, Jarling R, Beck A, Amann R, Wilkes H, Reinhardt R, Rabus R: Complete genome, catabolic sub-proteomes and key-metabolites of *Desulfobacula toluolica* Tol2, a marine, aromatic compound-degrading, sulfate-reducing bacterium. Environ Microbiol 2013;15:1334–1355.

Zedelius J, Rabus R, Grundmann O, Werner I, Brodkorb D, Schreiber F, Ehrenreich P, Behrends A, Wilkes H, Kube M, Reinhardt R, Widdel F: Alkane degradation under anoxic conditions by a nitrate-reducing bacterium with possible involvement of the electron acceptor in substrate activation. Environ Microbiol Rep 2011;3:125–135.

Zengler K, Heider J, Rosselló-Mora R, Widdel F: Phototrophic utilization of toluene under anoxic conditions by a new strain of *Blastochloris sulfoviridis*. Arch Microbiol 1999;172:204–212.

Zeyer J, Kuhn EP, Schwarzenbach RP: Rapid microbial mineralization of toluene and 1,3-dimethylbenzene in the absence of molecular oxygen. Appl Environ Microbiol 1986;52:944–947.